applied sciences

MDPI

Article

Precast Concrete Pavements of High Albedo to Achieve the Net "Zero-Emissions" Commitments

Miguel Ángel Sanjuán [1,*], Ángel Morales [2] and Aniceto Zaragoza [3]

[1] Spanish Institute of Cement and Its Applications (IECA), C/José Abascal, 53, 28003 Madrid, Spain
[2] Concentrating Solar Power Unit (CIEMAT), Avenida Complutense, 40, 28040 Madrid, Spain; angel.morales@ciemat.es
[3] Oficemen, C/José Abascal, 53, 28003 Madrid, Spain; azaragoza@oficemen.com
* Correspondence: masanjuan@ieca.es; Tel.: +34-914429166

Featured Application: Replacement of black pavements by high-reflective concrete pavements is an easy and cost-effective measure to stem climate change. In addition, concrete is a building material that is fully recyclable at the end of its service life. Furthermore, the construction of concrete pavements demands local resources, avoiding greenhouse gas emissions due to transport.

Abstract: Pavements store heat, which is subsequently released into the atmosphere, heating the surrounding air. Therefore, this process contributes to climate change and global warming. For this reason, the use of high-solar-reflectance (albedo) pavements is seen as one of the potential mitigation methods for climate change. Concrete pavements have a much higher albedo than asphalt due to their light gray color compared with black pavements. Accordingly, the widespread utilization of highly reflective concrete pavements will improve local climate change mitigation. Nevertheless, concrete albedo slightly decreases over time because of weathering. Albedo and solar reflectance index (SRI) measurements were taken on actual precast concrete pavements made with different mixes. The methodology applied for this project is based on the comparison between the asphalt and concrete pavements' reflectivity. Conventional concrete mix designs can provide cool pavements with SRI higher than 29. Replacement of black pavements by highly reflective concrete pavements appeared to be a cost-effective and easily implemented measure to combat climate change. Finally, multidisciplinary studies considering factors such as building materials' albedo, among other mitigation measures, should be performed to provide more precise and reliable guidance to policymakers, stakeholders, decision makers and urban planners.

Keywords: climate change; 1.5 °C climate goal; albedo; greenhouse gases; climate change policies

Citation: Sanjuán, M.Á.; Morales, Á.; Zaragoza, A. Precast Concrete Pavements of High Albedo to Achieve the Net "Zero-Emissions" Commitments. *Appl. Sci.* **2022**, *12*, 1955. https://doi.org/10.3390/app12041955

Academic Editor: Dario De Domenico

Received: 25 January 2022
Accepted: 11 February 2022
Published: 13 February 2022

1. Introduction

According to the law of conservation of energy, radiation of wavelength λ incident upon a material has either been transmitted across the material, has been reflected from its external surface or has been absorbed. The proportions of transmitted, reflected and absorbed energy can be expressed as ratios of the incident energy [1]. Accordingly, transmissivity (Ψ_λ), reflectivity (α_λ) and absorptivity (ζ_λ) are defined as dimensionless numbers between zero and the unity, according to Equation (1). They are radiative properties of the material. Strictly speaking, Equation (1) is valid exclusively for the case of a single wavelength. Nevertheless, it is acceptable for fairly wide range of wave bands. For instance, the reflectivity, α, for solar radiation, is referred to as the surface albedo. Therefore, surface albedo can be defined as the reflected solar radiation of the material surface divided by the amount incident upon it, and it is one of the main parameters of material surface radia-

tion [2]. Consequently, the value of the reflectivity, α, directly determines the absorptivity of an opaque surface.

$$\Psi_\lambda + \alpha_\lambda + \zeta_\lambda = 1, \quad (1)$$

Albedo regulates the surface short-wave absorption for a given solar input. This fact controls the daytime net radiation budget. Consequently, it rules the moisture and thermal climate of the material surface and the surrounding air and land. In particular, the albedo (α_λ) is a key surface characteristic and one which can be easily modified by surface treatment. Furthermore, it should be taken into account that some surfaces that are dark colored can reflect large portions of infrared solar radiation. Accordingly, they may also have high albedo values [3]. Modification of the construction material's albedo will invoke a significant climatic chain reaction [4].

The climatic conditions and the layout of the buildings has been a subject of interest since the 1st century BC, when Marco Lucio Vitruvio Polion showed that climatic conditions and the layout of the buildings should be considered by the architects [5]. Currently, it is widely acknowledged that the placement of a building on the landscape gives rise to moisture, thermal, radiative, and aerodynamic variation of the surrounding environment.

Although cities occupy just 2% of the Earth's land surface, city dwellers consume about 75% of the world's energy resources [6]. In addition, the urban population is increasing worldwide as more people are leaving the rural areas to move to the cities.

Albedo and land surface temperature (LST) are correlated [7], i.e., a high albedo value (high reflection rate of solar radiation) results in lower heat absorption, and therefore, in a lower LST value. Accordingly, the utilization of building materials with high values of albedo can help to reduce heat accumulation within cities [7]. Andrés-Anaya et al. [7] reported a temperature reduction and performance improvement of construction materials for Urban Heat Island (UHI) mitigation in the city of Valladolid (Spain). Taha [8] has argued that mitigation measures can offset the Urban Heat Island (UHI). Furthermore, the use of several simultaneous measures can further offset the UHI, albeit the combined results are not linear and normally smaller than the mere sum of cooling effects from the individual measures.

The main methods for retrieving information about Urban Heat Island (UHI) and albedo effect of pavements are numerical modelling, "in situ" measurements and remote sensing. The first one is the most widely used method, followed by "in situ" measurements and remote sensing [9]. Remote sensing is a promising method for retrieving information about the heat from the Earth's surface covering a large area, where satellites and aircrafts are used to collect images showing the data [10]. Some sensors capture the long- and short-wavelength radiant energy reflected from the Earth's surface [11,12]. For instance, the surface albedo in the entire land surface of Chinese has been assessed from 2000 to 2016 by using the database of the MODIS (Moderate Resolution Imaging Spectroradiometer) key instrument aboard the NASA's Terra satellite [13]. In addition, Geographic Information Systems (GIS) has been used to study the Urban Heat Island (UHI) effect in several cities in Greece [14], and in Shanghai [15], Singapore [16], Atlanta [17], and so on. Other studies are focussed on studying the impact of Urban Heat Islands (UHI) on population health [18].

Thermodynamic models based on thermal and radiative exchanges between the land surface and the atmosphere, and atmospheric models, which simulate local temperature distribution, are categorized as computer models. They are used to assess, simulate, and predict the thermal spatial distribution and energy flows.

Finally, the greatest advantage offered by the "in situ" measurements approach is the direct and reliable measurement of the physical parameters, such as land temperature, air temperature, humidity, wind speed and direction and energy flows, among other parameters [19].

According to new satellite imagery provided by international space agencies, urban pavements are important sources of heat radiation and thermal activity [6]. That is to say, pavements absorb solar energy and radiate it back to the atmosphere, contributing substantially to climate change.

Acharya et al. [20] performed computational fluid dynamics (CFD) analyses on asphalt and concrete pavements, and they concluded that increasing the albedo is more effective in reducing pavement surface temperatures than increasing the thermal inertia.

Soares et al. [21] underlined the significance of performing a particular assessment for each local area whenever an intervention is to be planned. They found that a higher pavement emissivity reduces both air and mean radiant temperatures. Nevertheless, pavement albedo results can be different between to mean radiant temperature reported in confined spaces and what tests reveal in larger and more open spaces. The albedo decrease in small spaces is due to radiation trapping within the canyons. Therefore, thermal conditions of outdoor areas can be affected by many factors, and climatic predictions are not that simple, but some tendencies can be identified in any case.

Pavements play a key role in the social and economic progress of the countries, which often entail significant improvements in the life of individuals. Therefore, pavements account for a considerable extension of the land cover worldwide. Overall, cool pavements are basically classified into three types: (i) reflective cool pavements, (ii) evaporative cool pavements, and (iii) heat storage pavements [22,23]. Recently, pavement solar collector (PSC) technology has been developed, whereby pavement heat is used for recharging geothermal boreholes [24].

The most common materials utilized for pavement construction are asphalt and concrete. It is well-known that conventional pavements can absorb and store solar radiation due to their dark and opaque surface and their large thermal inertia [25]. By contrast, the design and use of highly reflective pavements is a mitigation strategy which is gaining more interest regarding minimizing climatic change effects. Cotana et al. [26] reported a reduction of 16,000 tons of CO_{2eq} provided by a high-albedo surface area of 115,000 m^2 for a service life of 30 years. In addition, permeable pavements are more effective than traditional ones in reducing air temperature compared to the current asphalt surface [27].

Furthermore, some coated materials can be nearly 1 °C cooler for concrete and about 5 °C cooler for asphalt pavements [28]. Manni and Nicolini [29] suggested that the use of cool coatings can be optimized to improve urban albedo.

Accordingly, Zeng et al. [30] reported that high-albedo construction materials in urban areas are enough to alleviate high temperatures in megacities worldwide, such as Shenzhen and Hong Kong in China.

The albedo of some common materials used in pavement construction is given in Table 1, where it can be seen that in comparison with asphalt, they are rather high [31–35]. Concrete is a mix composed of Portland cement (grey or white) [36], aggregates, water, chemical admixtures, and sometimes supplementary cementitious materials (SCM) such as coal fly ash, blast-furnace slag and silica fume. Besides, the external concrete surface may be covered by a fine white layer of calcium carbonate formed by carbonation [37] or salts deposition (efflorescence). Albedo of smooth-surface concrete ranges from 0.41 to 0.77. Moreover, white-cement smooth concrete's albedo value is approximately 0.18–0.39 higher than that of grey-cement smooth concrete [31]. Nevertheless, abrasion, weathering and dirt reduce concrete albedo about 0.05-0.19. These albedo values are higher than albedo values found in many natural surfaces (e.g., desert is 0.35 and jungle is 0.12) [31]. Another way of fighting against climate change is the use of cost-effective new materials such as polymer wastes and nanofibers [38,39]. In addition, they could have a positive contribution to the concrete albedo.

The Leadership in Energy and Environmental Design (LEED) program for certifying the amount of sustainability incorporated in a building design is one of the most widely utilized green building rating systems in the world [40]. There are 110 points available through seven categories (base certification: 40–49; silver: 50–59; gold 60–79, and platinum > 80 points). One point can be scored in the credit 7.1 by using hardscape materials with an SRI of at least 29, such as conventional concrete pavements [41]. Additionally, 1–2 points could be scored under the materials and resources credit 4 for recycled content.

Table 1. Albedo of typical pavement materials and concrete constituents.

Pavement Constituent	Albedo
New asphalt	0.05–0.10
Polished asphalt	0.10–0.20
White Portland cement	0.87
Blast-furnace cements	0.71–0.75
Grey Portland cement	0.32–0.47
Coal fly ash	0.28–0.55
Fine grain natural gravel	0.62
Gold and white rock (chert, iron impurities)	0.55
White rock (plagioclase)	0.49
Limestone fine aggregate	0.42
Limestone coarse aggregate	0.42
Dark grey riverbed sand (quartz, clay minerals, mica)	0.20
Black and red rock (granite)	0.19
Concrete composed of ordinary Portland cement, fine aggregate fromcrushed limestone, and light-colored slag cement	0.64
Concrete composed of white cement and fine aggregate from crushed limestone	0.64
Smooth dry concrete made with white cement and fine aggregate from crushed limestone	0.41–0.77
New grey concrete	0.35–0.40
Weathered grey concrete	0.25–0.30

These points may be awarded if at least 10–20% of the total cost of the materials contains by-products and recycled materials. Some blended cements such as slag cements are considered in LEED as a material made with recycled constituents [40].

Climate change has become a central concern in local policy. In 2005, The C40 Cities Climate Leadership Group was founded. This is a network of mayors of about 100 world-leading cities worldwide working together to confront the climate change crisis. In 2020, 54 cities representing about 10% of the world's economy finalized climate action plans in line with avoiding climate change. In 2021, the C40′s Leadership Standards for 2021–2024, to ensure C40 are on the way to a zero-carbon future, went into effect. Furthermore, C40 partnered with The Global Cool Cities Alliance (GCCA), which was launched in 2010. One project of this group is the "100 Cool Cities" program that will endeavor to obtain commitments from 100 major cities worldwide and great implementation of cool pavements and roofs in a timely and predictable manner [42]. Considering that pavements and roofs comprise roughly 60% (normally, roofs account for 20–25%, whereas pavements for approximately 40%) of city surfaces, pavements and roofs with high solar reflectance could help to reflect away the summer temperatures of cities (Urban Heat Island, (UHI)), improving outdoor comfort by reducing summer air temperature by 2–3 °C.

The City of Madrid committed to ensuring that a large area of the city will be "zero-emission" by 2030, by signing the C40 Green and Healthy Streets Declaration on 9th December 2019. The specific objectives for each of the strategic objectives are defined within the context of the overall commitment of the Roadmap to Climate Neutrality by 2050. Within the strategic objective named "A cooler city", there is a specific objective to encourage the use of high-albedo building materials [43].

This paper is focused on testing reflective concrete pavements. Albedo and the solar reflectance index (SRI) of different precast concrete pavements have been measured. The results found in these concrete pavements are compared with the ones reported for the most commonly used materials to construct pavements. Finally, the effect of using high-albedo pavement materials on climate change mitigation has been discussed.

2. Materials and Methods

2.1. Pavement Materials for Measurement

Precast concrete pavements made by different materials and provided by one manufacturer (*QUADRO*, Casarrubuelos, Madrid, Spain) were used in this experimental program (Figure 1). Precast concrete pavement with improved mix designs can be considered as an emerging technology worldwide for climate change mitigation. These precast elements are perfect for use in innovative and functional pavement systems. Thereby, they aim to improve the mitigation procedures, engage more effective means of construction, and promote sound rehabilitation of existing pavements.

Figure 1. QUADRO samples from top to bottom: first column: Glacier 1 and 2; second column: Glacier 3 and 4; third column: Glacier 5 and 6; and fourth column: titanium and dolomite.

Precast concrete pavements were made with Portland cement CEM I 52.5 R according to the European standard for common cements, grey or white, depending on the final color of the sample. Siliceous and calcareous sand (0–2 mm) was used. The calcareous sand was marble powder. Table 2 collects the code and main characteristics of all the tested precast concrete pavements. They were made with different Portland cements and aggregates.

Table 2. Description and codification of the tested samples.

Code	Denomination and Description	Color
Glacier 1 and 2	Concrete slabs aged in a natural manner	Glacial grey tone
Glacier 3 and 4	Concrete slabs without ageing treatment and kept in factory	Glacial grey tone
Glacier 5 and 6	New mix design used in concrete slabs without ageing treatment	Glacial grey tone
Titanium	Concrete slabs without ageing treatment with high SRI index. Titanium colour	Clear grey with a slight white tinge
Dolomite	Concrete slabs without ageing treatment with high SRI index. Dolomite colour	Clear grey with a slight yellow tinge

2.2. Measurement Method and Equipment

Square prims were taken from precast pavements currently used in practice in Spain. Albedo average results (R_m), solar absorptance (α), thermal emittance (ε) and the temperature that each sample would reach (T_s) and its solar reflectance index (SRI) for three

convection coefficients (h_c), corresponding to three wind speeds, were measured in cut concrete surfaces. They were dried prior to radiative properties measurement because the moisture of the material markedly modifies the reflectance of concrete surfaces.

In order to calculate thermal emittance, hemispherical reflectance of pavements is measured with a single-beam FTIR Perkin Elmer Frontier Spectrophotometer, with a 75 mm integrating sphere coated with a gold diffusing material.

Four readings of each pavement samples were measured (2500–17,000 nm) and thermal emittance was calculated using hemispherical spectral reflectance ($\rho_{\lambda,h}$) with blackbody emission at 298 K:

$$\frac{\int_{0.3\mu m}^{17\mu m}(1-\rho_{\lambda,h})i_{\lambda,bb}(\lambda,T_a)d\lambda}{\int_{0.3\mu m}^{17\mu m} i_{\lambda,bb}(\lambda,T_a)d\lambda}$$

where $i_{\lambda bb}(\lambda,T_a)$ is the emission of a blackbody at ambient temperature.

Thermal emittance at a defined temperature T (εT) is the energy emitted by a material in comparison with the energy emitted by a blackbody at the same temperature and represents the ability of a material to lose energy by thermal radiation. Pavements with high emittance values will lose thermal energy faster than pavements with lower ones and they will reach lower temperatures by solar absorption.

Albedo, or solar reflectance, is the percentage of solar energy reflected by a surface. Researchers have developed methods to determine solar reflectance by measuring how well a material reflects energy at each wavelength, then calculating the weighted average of these values.

In order to calculate albedo, hemispherical reflectance of pavements is measured with a double-beam UV/VIS/NIR Perkin Elmer Lambda 950 Spectrophotometer, with a 10 cm integrating sphere coated with a diffusing material. The integrating sphere allows us to measure the amount of incident radiation on sample surface that is reflected in all directions.

Four readings of each pavement sample were measured (300–2500 nm), and albedos of concrete pavements were calculated by averaging reflectance measurements with air mass 1.5 global solar radiation spectrum:

$$Albedo = \frac{\int_{0.3\mu m}^{2.5\mu m} \rho_\lambda \, G_b(\lambda)d\lambda}{\int_{0.3\mu m}^{2.5\mu m} G_b(\lambda)d\lambda} \quad (2)$$

where ρ_λ is the hemispherical reflectance for each wavelength value and $G_b(\lambda)$ is the spectral solar irradiance AM1.5G (ASTM G173-03).

The air mass 1.5 albedo of a surface refers to its ability to reflect sunlight that has a spectral irradiance distribution characteristic of having traversed an atmospheric path length equal to 1.5 times the height of the Earth's atmosphere. This path length corresponds to a solar altitude of 42°. An air mass 1.5 irradiance is representative of average conditions in the contiguous United States (ASTM 1998) [44].

2.3. Solar Reflectance Index

The solar reflectance index (SRI) represents the "coolness" of a material surface, since it accounts for the two major characteristics, i.e., solar reflectance and thermal emittance. This index is determined according to the procedure described in the American standard ASTM 1980 [44]. Firstly, the steady-state surface temperature under the sunlight (T_s), the apparent sky temperature, T_{sky}, the solar absorbance, α, the irradiance, I, and the thermal emissivity, ε, are evaluated (Equation (3)).

$$\alpha \, I = \varepsilon \, \sigma \left(T_S^4 - T_{Sky}^4\right) + h_c \ (T_S - T_a) \quad (3)$$

where σ is the Stefan–Boltzmann constant (5.670367×10^{-8} W m^{-2} K^{-4}) and h_c is the convective coefficient (W m^{-2} K^{-1}). In addition, the steady-state surface temperature can be calculated by using Equation (4).

$$T_s = 309.07 + \frac{(1066.07\ \alpha - 31.98\ \varepsilon\ )}{(6.78\ \varepsilon + h_c)} - \frac{(890.94\alpha^2 + 2153.86\ \alpha\ \varepsilon\ )}{(6.78\ \varepsilon + h_c)^2} \quad (4)$$

Finally, the solar reflectance index (SRI) of a surface can be calculated by iteration from the solar reflectance and thermal emittance testing measurements for some defined convection conditions and T_s (Equation (5)), where T_w and T_b are the steady-state surface temperatures of the white and black reference surfaces, respectively.

$$SRI = 100\ \frac{T_b - T_s}{T_b - T_w} \quad (5)$$

The conditions are described in the American standard ASTM 1980 [44].

Considering medium wind conditions, the standard black material surface with zero solar reflectance index (SRI = 0) is characterized by solar reflectance and thermal emittance values of 0.05 and 0.9, respectively, whereas the standard white material surface has solar reflectance of 0.8 and thermal emittance of 0.9.

Accordingly, high values of thermal emittance and solar reflectance induce lower surface temperatures and higher SRI results. The solar reflectance index (SRI) could be considered as an indirect coolness scale where the fully reflective white material corresponds to an index equal to 100, and the fully absorptive black surface is characterized by an index equal to zero. Nevertheless, some new materials recently available in the building sector could be lower than 0 or higher than 100.

3. Results and Discussion

Solar reflectance is often measured in terms of albedo, and Figure 2 shows the four individual results considered in this work for each sample to calculate the average albedo, R_m. It should be stressed that the standard deviation for the samples with the highest albedo values (dolomite and titanium) was the lowest.

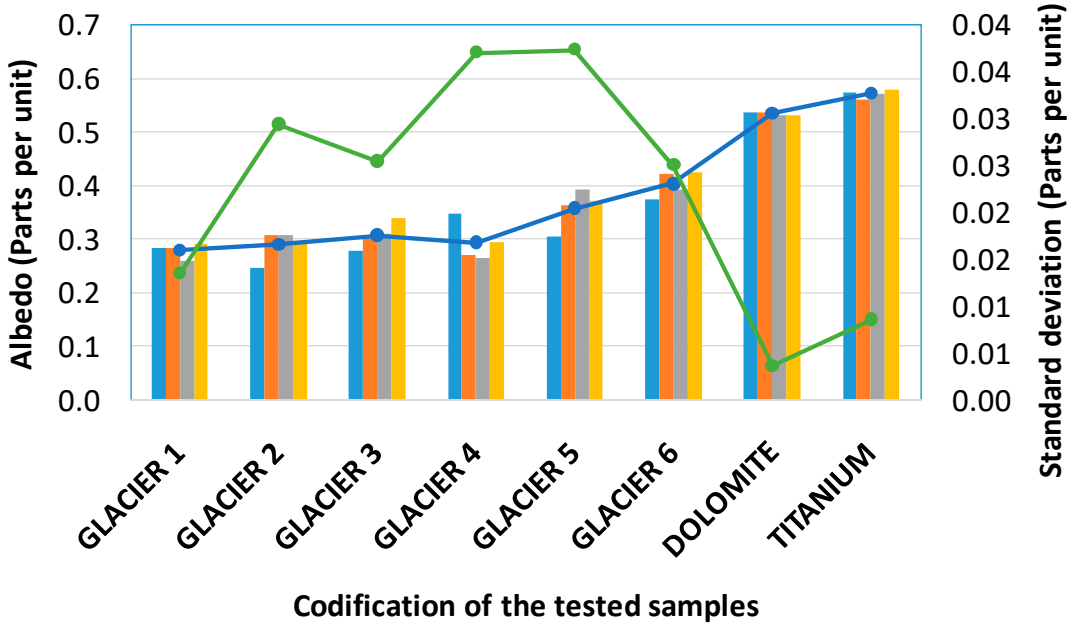

Figure 2. Individual albedo results (bars), average albedo, R_m (green line) and standard deviation (blue line).

Table 3 shows the albedo average results (R_m), solar absorptance (α), thermal emittance (ε), temperature that each sample would reach (T_s) and the solar reflectance index (*SRI)* for three convection coefficients (h_c), corresponding to three wind speeds, obtained in the tested precast pavements.

Table 3. Albedo average results (R_m), solar absorptance (α), thermal emittance (ε), the temperature that each sample would reach (T_s) and its solar reflectance index (*SRI*) for three convection coefficients (h_c), corresponding to three wind speeds.

Denomination	Rm	α	ε	*Ts* (hc = 5)	Ts (*hc* = 12)	Ts (hc = 30)	*SRI* (hc = 5)	SRI (hc = 12)	SRI (hc = 30)
BLACK	-	0.95	0.9	376.2	355.4	334.3	0.0	0.0	0.0
WHITE	-	0.2	0.9	322.2	318.0	313.9	100.0	100.0	100.0
GLACIER 1	0.281	0.719	0.897	360.6	344.2	328.1	28.9	29.8	30.3
GLACIER 2	0.291	0.709	0.894	360.0	343.8	327.8	30.1	30.9	31.5
GLACIER 3	0.309	0.691	0.888	359.0	343.0	327.4	32.0	33.0	33.8
GLACIER 4	0.295	0.705	0.888	359.9	343.7	327.8	30.2	31.2	31.9
GLACIER 5	0.359	0.641	0.882	355.6	340.6	326.1	38.2	39.4	40.3
GLACIER 6	0.404	0.596	0.886	352.2	338.3	324.8	44.5	45.6	46.4
DOLOMITE	0.535	0.465	0.891	342.5	331.6	321.2	62.5	63.5	64.1
TITANIUM	0.572	0.428	0.893	339.7	329.7	320.2	67.7	68.6	69.1

Average albedo values of all the samples range from 0.28 to 0.57, while solar absorptance values range from 0.42 to 0.72. In addition, solar absorptances for the white and black bodies were 0.2 and 0.95, respectively.

High-albedo concrete surfaces tend to keep the pavement environment cooler than low-albedo concrete surfaces by promoting a further takeaway in energy efficiency enhancement of the heat pumps because of the lower thermal gap [45].

Only three samples have albedo values below 0.30 (Glacier 1, Glacier 2 and Glacier 4). Glacier 1 and Glacier 2 correspond to the concrete slabs aged in a natural manner, while Glacier 3 and Glacier 4 are concrete samples without ageing. These paving materials were made with dark grey Portland cement and fine siliceous aggregates. The ageing effect is quite low, that is, the albedo fell from 0.30 to 0.28 in the worst-case scenario. Furthermore, the new mix design provides albedo values that can go as high as 0.36–0.40 (Glacier 5 and Glacier 6). In any case, concrete pavements have a much higher albedo than asphalt pavements due to their light gray color compared with black, but unfortunately, concrete albedo decreases over time because of weathering and the accumulation of dirt.

By contrast, the highest albedo was measured in the titanium sample (0.57), which was made with white Portland cement. This specimen shows a clear grey color with a slight white tinge. The second highest albedo was recorded in the dolomite pavement (0.54), which was made with grey Portland cement. In this case, it presents a clear grey color with a slight yellow tinge.

Figure 3 shows the solar reflectance index (SRI) as a function of the wavelength. Dolomite and titanium samples present a maximum SRI between 50 and 60 in the range between 500 and 1500 nm, whereas there was a downward trend in the samples with the lowest albedo (from 30–35 to 20) in the same range of wavelengths.

There is a linear correlation between the solar reflectance index (SRI) and albedo. Figure 4 shows the marked correlation between the SRI and albedo. As the trend line shows, there is a significant correlation between the two. The following Equations (6)–(8) show the strong correlation ($R^2 > 0.999$).

$$\text{For } h_c = 5\text{: } y = 134.03x - 9.2667;\ R^2 = 0.9993 \quad (6)$$

$$\text{For } h_c = 12\text{: } y = 133.81x - 8.1937;\ R^2 = 0.9997 \quad (7)$$

$$\text{For } h_c = 30\text{; } y = 133.59x - 7.4259;\ R^2 = 0.9999 \quad (8)$$

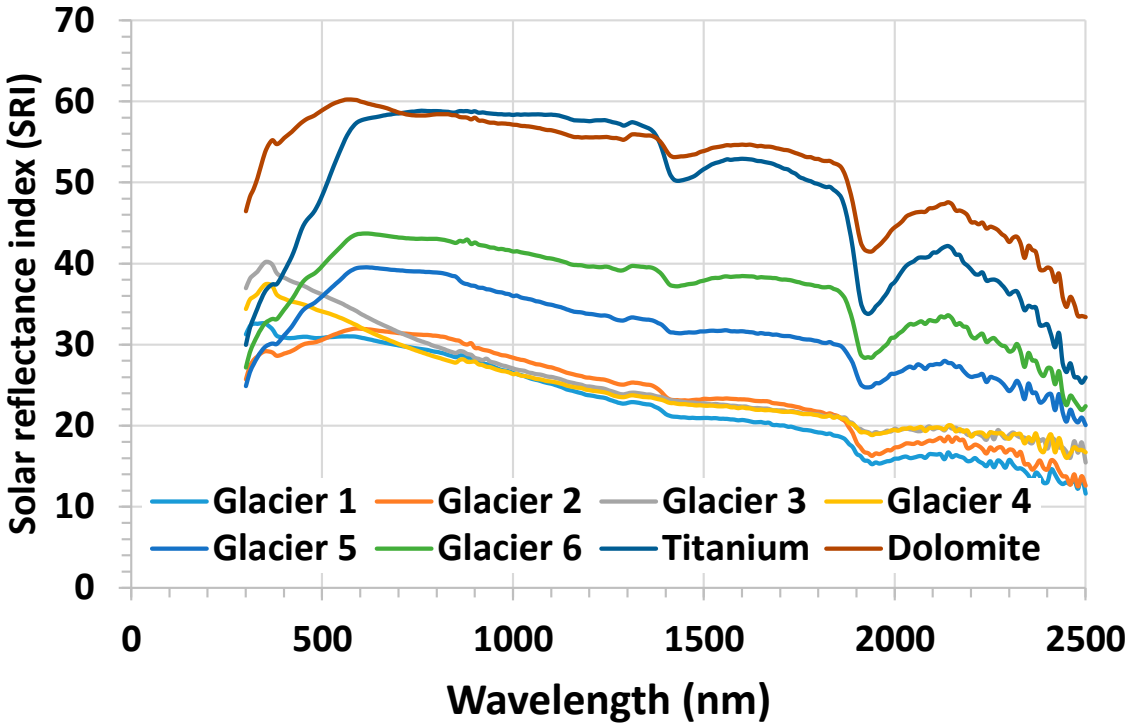

Figure 3. Solar reflectance index (SRI) as a function of the wavelength.

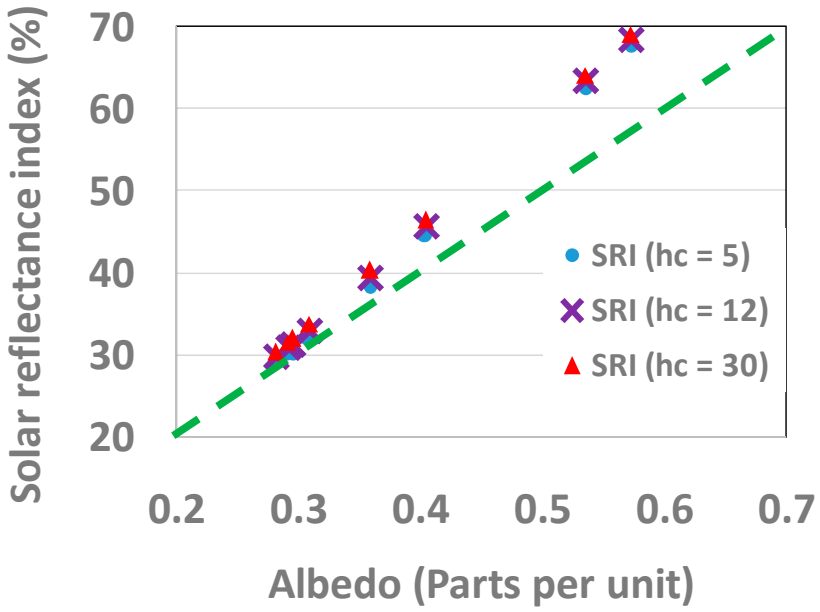

Figure 4. Correlation between the solar reflectance index (SRI) and albedo.

The Wanda Metropolitano Stadium in Madrid, Spain, was built between 1990–1993 with Glacier precast concrete pavements (Figure 5). Precast concrete pavement named Glacier was collocated into the surrounding ground with a solar reflectance index (SRI) about 0–30 and albedo 0.28–0.29 (Table 3). It has been estimated that ageing will reduce concrete albedo of this pavement by about 0.1.

Figure 5 shows several pavement applications of the tested precast pavements with their albedo values: (a) Wanda Stadium (0.30); (b) titanium precast concrete pavement (0.57); (c) dolomite precast concrete pavement (0.54). The photograph on the left is a pavement made with white cement and a very fine and clear aggregate (dolomite precast concrete

pavement). Consequently, it presents a very high albedo of 0.54. The second photograph also shows an example of high-reflectance concrete pavement with a solar reflectance index (SRI) of 0.68–0.69 and albedo of 0.54 (Table 3). In fact, the use of cool-colored materials, namely titanium and dolomite (Figure 5b,c), increases albedo substantially without altering visual appearance.

(**a**) (**b**) (**c**)

Figure 5. Albedo in some pavement applications: (**a**) Wanda 1 (0.30); (**b**) Titanium (0.57); (**c**) Dolomite (0.54).

Typical albedo values for new concrete range between 0.35 and 0.40, and between 0.25 and 0.30 for weathered concrete [4]. For comparison, the common albedo value for asphalt is 0.05–0.10, which increases to about 0.10–0.20 over time due to the polishing effect of vehicular traffic and the subsequent exposure of aggregates.

The effect of decreasing albedo and SRI of precast concrete pavements with age can be observed clearly in Table 3. The new mix design (Glacier 5 and 6) of concrete sections appears much lighter (0.59–0.64) than the existing aged concrete (Figure 1). Although precast concrete pavements start out with a relatively high albedo, i.e., solar reflectance (Glacier 3 and 4), and are not as prevalent as asphalt in pavements, it is a worthwhile endeavour to improve the solar reflectance of pavements. Some research studies reported that even a small increase of 0.01 in albedo has an important environmental benefit. Therefore, it is recommended to use cool pavements (i.e., concrete pavements), which have made an effective contribution to climate change mitigation by reducing the Earth's surface temperature. Considering an albedo of 0.10 for asphalt pavements as reference value, we can calculate the "carbon dioxide equivalent" reduction by replacing this conventional type of pavement with concrete pavements. An increase in albedo of 0.1 causes a variation of 34.1 W m^{-2} and an average decrease in "carbon dioxide equivalent" of 25 $kgCO_2/m^2$ of pavement. Table 4 shows the reduction in carbon dioxide emissions by using the tested concrete pavements, taking as a reference the asphalt pavement's albedo.

Madrid Central is a low-emission zone located in the center of Madrid (4.72 km^2). More specifically, in the hypothetical case that it could be covered with high-reflectance materials (albedo > 0.5), a yearly equivalent reduction in carbon dioxide of 0.43 gigatons could be reached.

The stadium was built on 88,150 m^2 of land near the city center. The use of concrete pavements of albedo 0.30 instead of asphalt pavements will contribute to combatting climatic change by reducing about 4500 tons of carbon dioxide each year. This positive effect could be increased by using high-reflective concrete pavements with albedos over

0.5. In this case, the mitigation will become 8800 tons of carbon dioxide by pavement areas of 88,000 m^2 (Table 4).

Table 4. Reduction in carbon dioxide emissions by using the tested concrete pavements with different albedo values (R_m) calculated taking as a reference the asphalt pavements albedo.

Parameter	GLACIER 1	GLACIER 2	GLACIER 3	GLACIER 4	GLACIER 5	GLACIER 6	DOLOMITE	TITANIUM
Rm	0.281	0.291	0.309	0.295	0.359	0.404	0.535	0.572
Reduction in solar flux (W m^{-2})	61.72	65.13	71.27	66.50	88.32	103.66	148.34	160.95
Reduction in CO_2 ($kgCO_2/m^2$)	45.25	47.75	52.25	48.75	64.75	76	108.75	118
Reduction in CO_2 ($kgCO_2$) *	3,982,000	4,202,000	4,598,000	4,290,000	5,698,000	6,688,000	9,570,000	10,384,000

* Reduction in carbon dioxide emissions for 88,000 m^2 of concrete pavement ($kgCO_2$).

Climate change is having an alarming impact worldwide and the problem continues to grow because of ever-increasing global temperatures. Accordingly, extreme weather events are becoming more common.

Atmospheric carbon dioxide levels reached more than 400 parts per million. Therefore, urgent action is needed to combat climate change and to reduce the ever-increasing climate-related hazards. Albedo of the tested precast concrete pavements can be up to six times higher than that of asphalt pavements (Table 3). Thus, they reflect between 60 and 160 W m^{-2} of the incident radiation with respect to asphalt pavements. Accordingly, a reduction in the Earth's surface temperature, equivalent to a decrease of 45–118 $kgCO_2/m^2$, is expected.

4. Conclusions

From albedo and solar reflectance index (SRI) measurements on actual precast concrete pavements made with different mixes, the following qualitative takeaways are provided:

1. The tested precast concrete pavements present a range of solar reflectance values of 0.29–0.46. Therefore, all of them meet the requirements of LEED-NC SS 7.1 (SRI $\geq$ 29). Conventional concrete mix designs can provide cool pavements with SRI higher than 29. Replacement of black pavements by high-reflective concrete pavements is an easy and cost-effective measure to stem climate change.
2. There is a linear correlation between the solar reflectance index (SRI) and albedo.
3. It is estimated that the concrete mixes reflect between 60 and 160 W m^{-2} of the incident radiation with respect to dark conventional pavements, equivalent to a reduction of 45–118 $kgCO_2/m^2$. The main outcome of this carbon dioxide decrease is a reduction in Earth's surface temperature.
4. High-albedo (>0.5) concrete surfaces exhibit significant "active cool effects" due to a reduction in solar flux of 136 W m^{-2}, with an equivalent carbon dioxide emission reduction of 100 $kgCO_2/m^2$.
5. These results will allow stakeholders and decision makers to improve environmental resilience at large territorial scales, especially in the urban core.
6. Multidisciplinary studies considering factors such as building materials' albedo, among other mitigation measures, should be performed to provide more precise and reliable guidance to policymakers, stakeholders, decision makers and urban planners.
7. A huge surface of covered with 4.72 km^2 of high-reflectance materials (albedo > 0.5) can offset about 0.43 gigatons of carbon dioxide every year. Thus, concrete pavements can contribute very efficiently to climate change mitigation by lowering the land area temperature.
8. Concrete is fully recyclable material used to construct pavements, which is manufactured with local resources and may be successfully utilized for cool concrete pavement construction, replacing conventional asphalt pavements.

The novelty of this paper relies on the study of precast pavements founded on high-albedo constituents, which were disposed in actual places. They offer the possibility of continuous and more flexible supervision during the pavement's service life.

Author Contributions: Conceptualization, A.Z., M.Á.S. and Á.M.; methodology, Á.M. and M.Á.S.; software, Á.M. and M.Á.S.; validation, Á.M. and M.Á.S.; formal analysis, Á.M. and M.Á.S.; investigation, A.Z., M.Á.S. and Á.M.; resources, A.Z.; data curation, Á.M. and M.Á.S.; writing—original draft preparation, M.Á.S.; writing—review and editing, M.Á.S. and Á.M.; visualization, A.Z., M.Á.S. and Á.M.; supervision, A.Z.; project administration, A.Z.; funding acquisition, A.Z. All authors have read and agreed to the published version of the manuscript.

Funding: This research received no external funding.

Institutional Review Board Statement: Not applicable.

Informed Consent Statement: Not applicable.

Acknowledgments: The authors would like to thank the following people who assisted in providing the samples and technical data to perform the experimental presented in this paper: Luis Miguel Valle, QUADRO.

Conflicts of Interest: The authors declare no conflict of interest.

References

1. Irvine-Fynn, T.D.L.; Bunting, P.; Cook, J.M.; Hubbard, A.; Barrand, N.E.; Hanna, E.; Hardy, A.J.; Hodson, A.J.; Holt, T.O.; Huss, M.; et al. Temporal Variability of Surface Reflectance Supersedes Spatial Resolution in Defining Greenland's Bare-Ice Albedo. *Remote Sens.* **2022**, *14*, 62. [CrossRef]
2. Gul, M.; Kotak, Y.; Muneer, T.; Ivanova, S. Enhancement of Albedo for Solar Energy Gain with Particular Emphasis on Overcast Skies. *Energies* **2018**, *11*, 2881. [CrossRef]
3. Berdahl, P.; Bretz, S.E. Preliminary survey of the solar reflectance of cool roofing materials. *Energy Build.* **1997**, *25*, 149–158. [CrossRef]
4. Sanjuán, M.Á.; Morales, Á.; Zaragoza, A. Effect of Precast Concrete Pavement Albedo on the Climate Change Mitigation in Spain. *Sustainability* **2021**, *13*, 11448. [CrossRef]
5. Vitruvio, M.L. Climatic Conditions and the Layout of Buildings, 6th Book. In *On Architecture*, Vitruvius; Edited from the Harleian Manuscript 2767 and translated into English by Frank Granger, Loeb Classical Library; Chapter 1, 1st ed.; Harvard University Press: Cambridge, MA, USA, 1983–1985; p. 0674992776.
6. Madlener, R.; Sunak, Y. Impacts of urbanization on urban structures and energy demand: What can we learn for urban energy planning and urbanization management? *Sustain. Cities Soc.* **2011**, *1*, 45–53. [CrossRef]
7. Andrés-Anaya, P.; Sánchez-Aparicio, M.; del Pozo, S.; Lagüela, S. Correlation of Land Surface Temperature with IR Albedo for the Analysis of Urban Heat Island. *Eng. Proc.* **2021**, *8*, 9. [CrossRef]
8. Taha, H. Development of an Urban Heat Mitigation Plan for the Greater Sacramento Valley, California, a Csa Koppen Climate Type. *Sustainability* **2021**, *13*, 9709. [CrossRef]
9. Kong, J.; Zhao, Y.; Carmeliet, J.; Lei, C. Urban Heat Island and Its Interaction with Heatwaves: A Review of Studies on Mesoscale. *Sustainability* **2021**, *13*, 10923. [CrossRef]
10. Bahi, H.; Mastouri, H.; Radoine, H. Review of methods for retrieving urban heat islands. *Mater. Today Proc.* **2020**, *27*, 3004–3009. [CrossRef]
11. Li, S.; Liu, Y.; Pan, Y.; Li, Z.; Lyu, S. Integrating Remote-Sensing and Assimilation Data to Improve Air Temperature on Hot Weather in East China. *Remote Sens.* **2021**, *13*, 3409. [CrossRef]
12. Chen, C.; Tian, L.; Zhu, L.; Zhou, Y. The Impact of Climate Change on the Surface Albedo over the Qinghai-Tibet Plateau. *Remote Sens.* **2021**, *13*, 2336. [CrossRef]
13. Yuan, J. Investigation of Spatial and Temporal Changes in the Land Surface Albedo for the Entire Chinese Territory. *Geosciences* **2020**, *10*, 362. [CrossRef]
14. Stathopoulou, M.; Cartalis, C. Daytime urban heat islands from Landsat ETM+ and Corine land cover data: An application to major cities in Greece. *Sol. Energy* **2007**, *81*, 358–368. [CrossRef]
15. Li, J.; Wang, X.; Wang, X.; Ma, W.; Zhang, H. Remote sensing evaluation of urban heat island and its spatial pattern of the Shanghai metropolitan area, China. *Ecol. Complex.* **2009**, *6*, 413–420. [CrossRef]
16. Kardinal Jusuf, S.; Wong, N.H.; Hagen, E.; Anggoro, R.; Hong, Y. The influence of land use on the urban heat island in Singapore. *Habitat. Int.* **2007**, *31*, 232–242. [CrossRef]
17. Stone, B.; Rodgers, M.O. Urban form and thermal efficiency: How the design of cities influences the urban heat island effect. *J. Am. Plann. Assoc.* **2001**, *67*, 186–198. [CrossRef]

18. Tomlinson, C.J.; Chapman, L.; Thornes, J.E.; Baker, C.J. Including the urban heat island in spatial heat health risk assessment strategies: A case study for Birmingham, UK. *Int. J. Health Geogr.* **2011**, *10*, 42. [CrossRef] [PubMed]
19. Zhang, Y.; Wei, P.; Wang, L.; Qin, Y. Temperature of Paved Streets in Urban Mockups and Its Implication of Reflective Cool Pavements. *Atmosphere* **2021**, *12*, 560. [CrossRef]
20. Acharya, T.; Riehl, B.; Fuchs, A. Effects of Albedo and Thermal Inertia on Pavement Surface Temperatures with Convective Boundary Conditions—A CFD Study. *Processes* **2021**, *9*, 2078. [CrossRef]
21. Soares, R.; Corvacho, H.; Alves, F. Summer Thermal Conditions in Outdoor Public Spaces: A Case Study in a Mediterranean Climate. *Sustainability* **2021**, *13*, 5348. [CrossRef]
22. Qin, Y. A review on the development of cool pavements to mitigate urban heat island effect. *Renew. Sustain. Energy Rev.* **2015**, *52*, 445–459. [CrossRef]
23. Santamouris, M.; Gaitani, N.; Spanou, A.; Saliari, M.; Giannopoulou, K.; Vasilakopoulou, K.; Kardomateas, T. Using cool paving materials to improve microclimate of urban areas design realization and results of the flisvos project. *Build. Environ.* **2012**, *53*, 128–136. [CrossRef]
24. Johnsson, J.; Adl-Zarrabi, B. A numerical and experimental study of a pavement solar collector for the northern hemisphere. *Appl. Energy* **2020**, *260*, 114286. [CrossRef]
25. Cheela, V.R.S.; John, M.; Biswas, W.; Sarker, P. Combating Urban Heat Island Effect—A Review of Reflective Pavements and Tree Shading Strategies. *Buildings* **2021**, *11*, 93. [CrossRef]
26. Cotana, F.; Rossi, F.; Filipponi, M.; Coccia, V.; Pisello, A.L.; Bonamente, E.; Cavalaglio, G. Albedo control as an effective strategy to tackle Global Warming: A case study. *Appl. Energy* **2014**, *130*, 641–647. [CrossRef]
27. Moretti, L.; Cantisani, G.; Carpiceci, M.; D'Andrea, A.; Del Serrone, G.; Di Mascio, P.; Loprencipe, G. Effect of Sampietrini Pavers on Urban Heat Islands. *Int. J. Environ. Res. Public Health* **2021**, *18*, 13108. [CrossRef]
28. Lu, Y.; Rahman, M.A.; Moore, N.W.; Golrokh, A.J. Lab-Controlled Experimental Evaluation of Heat-Reflective Coatings by Increasing Surface Albedo for Cool Pavements in Urban Areas. *Coatings* **2022**, *12*, 7. [CrossRef]
29. Manni, M.; Nicolini, A. Optimized Cool Coatings as a Strategy to Improve Urban Equivalent Albedo at Various Latitudes. *Atmosphere* **2021**, *12*, 1335. [CrossRef]
30. Zeng, F.F.; Feng, J.; Zhang, Y.; Tsou, J.Y.; Xue, T.; Li, Y.; Li, R.Y.M. Comparative Study of Factors Contributing to Land Surface Temperature in High-Density Built Environments in Megacities Using Satellite Imagery. *Sustainability* **2021**, *13*, 13706. [CrossRef]
31. Levinson, R.; Akbari, H. Effects of composition and exposure on the solar reflectance of Portland cement concrete. *Cem. Concr. Res.* **2002**, *32*, 1679–1698. [CrossRef]
32. Boriboonsomsin, K.; Reza, F. Mix design and benefit evaluation of high solar reflectance concrete for pavements. *Transp. Res. Rec.* **2007**, *2011*, 11–20. [CrossRef]
33. Tsoka, S.; Tsikaloudaki, K.; Theodosiou, T.; Bikas, D. Urban Warming and Cities' Microclimates: Investigation Methods and Mitigation Strategies—A Review. *Energies* **2020**, *13*, 1414. [CrossRef]
34. Pisello, A.L.; Pignatta, G.; Castaldo, V.L.; Cotana, F. Experimental Analysis of Natural Gravel Covering as Cool Roofing and Cool Pavement. *Sustainability* **2014**, *6*, 4706–4722. [CrossRef]
35. Marceau, M.L.; VanGeem, M.G. *Solar Reflectance of Concretes for LEED Sustainable Sites Credit: Heat Island Effect*; SN2982; Portland Cement Association: Skokie, IL, USA, 2007; pp. 1–22.
36. Sanjuán, M.Á.; Suarez-Navarro, J.A.; Argiz, C.; Mora, P. Assessment of radiation hazards of white and grey Portland cements. *J. Radioanal. Nucl. Chem.* **2019**, *322*, 1169–1177. [CrossRef]
37. Sanjuán, M.Á.; Esteban, E.; Argiz, C.; del Barrio, D. Effect of curing time on granulated blast-furnace slag cement mortars carbonation. *Cem. Concr. Compos.* **2018**, *90*, 257–265. [CrossRef]
38. Saleh, H.M.; El-Sheikh, S.M.; Elshereafy, E.E.; Essa, A.K. Performance of cement-slag-titanate nanofibers composite immobilized radioactive waste solution through frost and flooding events. *Constr. Build. Mater.* **2019**, *223*, 221–232. [CrossRef]
39. Saleh, H.M.; Eskander, S.B. Impact of water flooding on hard cement-recycled polystyrene composite immobilizing radioactive sulfate waste simulate. *Constr. Build. Mater.* **2019**, *222*, 522–530. [CrossRef]
40. U.S. Green Building Council. Available online: https://www.usgbc.org/credits/core-shell-healthcare-new-construction-schools/v2009/ssc71 (accessed on 20 December 2021).
41. U.S. Green Building Council. LEED Rating System. Available online: https://www.usgbc.org/leed (accessed on 20 December 2021).
42. Global Cool Cities Alliance (GCCA). A Practical Guide to Cool Roofs and Cool Pavements. January 2012. p. 85. Available online: https://globalcoolcities.org/ (accessed on 20 December 2021).
43. Madrid 360. Roadmap to Climate Neutrality by 2050. p. 60. Available online: https://www.madrid.es/UnidadesDescentralizadas/Sostenibilidad/EspeInf/EnergiayCC/06Divulgaci%C3%B3n/6cDocumentacion/6cNHRNeutral/Ficheros/RoadmapENG.pdf (accessed on 22 December 2021).
44. American Society for Testing and Materials (ASTM). *ASTM C1980: Standard Practice for Calculating Solar Reflectance Index of Horizontal and Low-Sloped Opaque Surfaces*; American Society for Testing and Materials: West Conshohocken, PA, USA, 2011.
45. Pisello, A.L.; Santamouris, M.; Cotana, F. Active cool roof effect: Impact of cool roofs on cooling system efficiency. *Adv. Build. Energy Res.* **2013**, *7*, 209–221. [CrossRef]